Reliable GNSS Joint Position and Attitude Estimation in Harsh Environments through Robust Statistics

Andrea Belles, Daniel Medina, Paul Chauchat, Jordi Vila-Valls

Reliable GNSS Joint Position and Attitude Estimation in Harsh Environments through Robust Statistics

Andrea Bellés[(1)], Daniel Medina[(1)], Paul Chauchat[(2)] and Jordi Vilà-Valls[(2)]
[(1)] **Institute of Communications and Navigation, German Aerospace Center (DLR), Germany.**
[(2)] **ISAE-SUPAERO/University of Toulouse, Toulouse, France.**

***Abstract*— Next-generation navigation systems require precise and robust solutions, providing information about both the system position and its attitude, of particular interest in intelligent transportation systems and robotics applications. Within this context, Global Navigation Satellite Systems (GNSS) are the main source of positioning data and, in multiple antenna setups, can also provide attitude information. Notice that the use of phase observables is mandatory to obtain a precise solution. In this contribution, we leverage the recently introduced recursive GNSS joint position and attitude (JPA) estimation framework, which has been shown to provide good performance under nominal conditions. The main goal is to further elaborate the JPA problem and to propose a new robust filtering solution able to mitigate the impact of possible outliers, which may otherwise cause a performance breakdown of standard JPA, because of the sensitivity of carrier phase measurements. Illustrative results are provided to support the discussion and show the performance improvement of the proposed approach.**

TABLE OF CONTENTS

1. INTRODUCTION

Next-generation navigation systems require *robust* and *precise* solutions, two performance criteria that may not be easy to achieve simultaneously. Within the large navigation field, Global Navigation Satellite Systems (GNSS) are the main source of positioning data for a wide range of applications [1]. If using multiple antenna setups, GNSS can in addition be exploited for attitude determination and/or joint position and attitude (JPA) estimation, of particular interest in aerospace, for satellite orbit determination [2–4], and outdoor navigation in vehicular and robotics applications [5–8]. In such applications, it is fundamental to ensure a reliable precise positioning solution, able to operate in harsh propagation conditions such as urban environments, which implies coping with multipath and other non-nominal disturbances.

This brings a fundamental dilemma: while carrier phase measurements must be used to obtain a precise solution, such observables and the corresponding integer ambiguity resolution are particularly sensitive to non-nominal conditions (i.e., much more than code-based observables). This limits the applicability of carrier phase-based positioning techniques (e.g., Real-Time Kinematic (RTK) or Precise Point Positioning (PPP)) in challenging scenarios, the reason why new robust solutions must be accounted for.

Similarly, the use of multi-antenna configurations, together with carrier phase observables, allows to provide precise estimates on the target platform's orientation. While a rich literature on GNSS-based attitude determination exists [5, 9–11], its estimation is typically decoupled from the positioning problem. The first proposal for its combined estimation can be found in Array-PPP [12], which provides a batch least squares (LS) solution for the PPP and attitude problems. More recently, a recursive Kalman filter (KF)-based approach was proposed [13], leveraging on the algebra of the Lie group to provide an enhanced availability and precision of the navigation solution. The performance degradation of such JPA in harsh propagation conditions, and possible ways to cope with it, has not yet been reported in the literature.

A possible way to account for non-nominal conditions at the observable level (i.e., propagation effects which deviate from the Gaussianity assumption) is to consider the typical contamination model arising in robust statistics: a proportion of observations under nominal Gaussian-distributed noise, and another proportion of observations contaminated by an arbitrary unknown distribution accounting for possible outliers (i.e., corrupted observations). In that perspective, a plethora of batch (robust LS-type) and recursive (robust KF-like) estimation techniques exist in the literature to detect, reject, or mitigate the impact of potentially faulty measurements. These techniques have been successfully applied both in the context of code-based and RTK positioning [14–18], and have been shown to be a promising solution.

Within the context of multi-antenna carrier phase-based navigation, the goal of this contribution is to further elaborate on the framework of robust filtering. Hence, a robust quaternion-parametrized KF-based filtering approach is proposed, able to mitigate the impact of outlying observations, therefore, combining and generalizing the previous results in [18] and [13]. For the purpose of simplicity, and since it is independent from the filtering part, the integer ambiguity resolution (IAR) process (i.e., the procedure to map the real-valued ambiguities to integer ones) which follows the filtering estimation is beyond the scope of this work. Illustrative results are provided to support the discussion and show the performance improvement with respect to state-of-the-art solutions.

The article is organized as follows: the JPA problem is introduced in Sec. 2, and background on nonlinear/robust filtering in Sec. 3. The new robust filter formulation for JPA is provided in Sec. 4, and numerical results in Sec. 5.

2022 IEEE Aerospace Conference (AERO) | 978-1-6654-3760-8/22/$31.00 ©2022 IEEE | DOI: 10.1109/AERO53065.2022.9843300

2. Background on GNSS JPA Estimation

Addressing the complete dynamics for a platform implies the estimation of its orientation, velocity and position. GNSS-based JPA estimation concerns the use of GNSS carrier phase observations along an array of $N+1$ antennas installed on a vehicle, and a nearby base station of known coordinates, as illustrated in Fig. 1. This section briefly introduces the JPA estimation problem as it was proposed in [13]. In particular its state-space model is described together with the system dynamics and observation model.

General State-Space Model Formulation

Consider a discrete state-space model (SSM) described by the evolution of the states over time, through a *process model* $\mathbf{f}(\cdot)$, and the relationship of these to the observations, through an *observation model* $\mathbf{h}(\cdot)$, as

$$\mathbf{x}_k = \mathbf{f}\left(\mathbf{x}_{k-1}, \boldsymbol{\omega}_{k-1}, \mathbf{w}_{k-1}\right), \tag{1}$$
$$\mathbf{y}_k = \mathbf{h}\left(\mathbf{x}_k\right) + \boldsymbol{\eta}_k, \tag{2}$$

with $\boldsymbol{\omega}_{k-1}$ the angular rates measured at epoch k by an IMU, $\mathbf{w}_{k-1} \sim \mathcal{N}(\mathbf{0}, \mathbf{Q}_{k-1})$ the process noise and $\boldsymbol{\eta}_k \sim \mathcal{N}(\mathbf{0}, \boldsymbol{\Sigma}_k)$ the (nominal) measurement noise. The state of the system is given by

$$\begin{aligned} \mathbf{x}_k^\top &= \left[\mathbf{q}_k^\top, \mathbf{a}_k^\top, \mathbf{p}_k^\top, \mathbf{v}_k^\top, \mathbf{b}_{k,\omega}^\top\right], \\ \mathbf{x}_k &\in \mathcal{S}^3 \times \mathbb{Z}^M \times \mathbb{R}^3 \times \mathbb{R}^3 \times \mathbb{R}^3, \end{aligned} \tag{3}$$

where $\mathbf{q}_k$ denotes the unit-norm quaternion rotation from the body to the (global) navigation frame –denoted with subscripts $\mathcal{B}$ and $\mathcal{G}$ respectively–, $\mathbf{a}_k$ is the vector of carrier phase integer ambiguities, $\mathbf{p}_k, \mathbf{v}_k$ are the position and speed respectively, and $\mathbf{b}_{\omega,k}$ is the gyroscope bias of the IMU. In this work, only gyroscope measurements are taken into account, for the sake of simplicity. Therefore, a constant velocity model is assumed (i. e., the acceleration is not contemplated in the model) and only gyroscope biases are estimated. Including the linear speed and gyroscope bias in the state vector allows taking into account the dynamics of the receiver, through the SSM process equation. The integer ambiguities are of dimension $M = n \cdot (N+1)$, considering $n+1$ GNSS tracked satellites over $N+1$ antennas installed on the vehicle. In general, the recursive estimation of $\mathbf{x}_k$, given measurements up to time k, $\mathbf{y}_{1:k}$, for nonlinear models as in (1)-(2), is typically tackled by nonlinear KF-type solutions or sequential Monte Carlo methods. Due to the presence of the quaternion and integer ambiguities, JPA requires specific treatments.

The complete JPA pipeline, following the standard RTK procedure [1], is a three-part process. During the first one, the integer constraint of the ambiguities is relaxed and they are estimated as real values. The two subsequent steps aim at recovering the actual integer values and correcting the state accordingly, leading to a significant precision gain. These three steps are described in [13]. This work focuses on the first filtering step. Therefore, the ambiguities will be considered as real-valued for the remainder of the paper. This means that we will consider

$$\begin{aligned} \mathbf{x}_k^\top &= \left[\mathbf{q}_k^\top, \mathbf{a}_k^\top, \mathbf{p}_k^\top, \mathbf{v}_k^\top, \mathbf{b}_{k,\omega}^\top\right], \\ \mathbf{x}_k &\in \mathcal{S}^3 \times \mathbb{R}^M \times \mathbb{R}^3 \times \mathbb{R}^3 \times \mathbb{R}^3 = \mathcal{M}. \end{aligned} \tag{4}$$

Recursive attitude estimation must also take into account and respect its inherent nonlinear geometric constraints –either the orthogonality and unit determinant for the rotation matrix

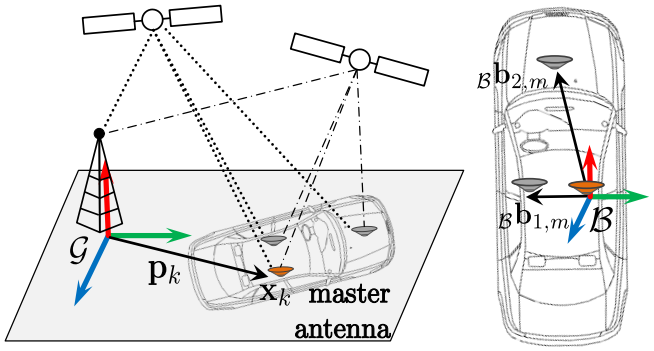

Figure 1. On the left, illustration for the GNSS-based JPA problem: the base station, the rover with multiple antennas. On the right, the configuration of the sensors on the body frame. The master antenna is highlighted in orange color.

or the unit norm for the quaternion– [19, 20]. This is now a well-known problem, typically addressed by geometric tools such as Lie group theory [21]. A possible solution is given by the so-called Error State KF (ESKF) –also known as Indirect KF– [22, 23], for which the state to be estimated $\mathbf{x}$ belongs to a manifold and its perturbations $\delta\mathbf{x}$ "live" in the tangent space of that manifold. Thus, the unknown true state is formulated as the composition of the nominal estimate $\widehat{\mathbf{x}}$ and the error state $\delta\mathbf{x}$, noted $\mathbf{x} = \widehat{\mathbf{x}} \oplus \delta\mathbf{x}$, and defined by (7), with the error state described by

$$\begin{aligned} \delta\mathbf{x}_k^\top &= \left[\delta\boldsymbol{\psi}_k^\top, \delta\mathbf{a}_k^\top, \delta\mathbf{p}_k^\top, \delta\mathbf{v}_k^\top, \delta\mathbf{b}_{\omega,k}^\top\right], \\ \text{with } \delta\mathbf{x}_k &\in \mathbb{R}^3 \times \mathbb{R}^M \times \mathbb{R}^3 \times \mathbb{R}^3 \times \mathbb{R}^3, \end{aligned} \tag{5}$$

and $\delta\boldsymbol{\psi}_k$ the rotation vector. The Euclidean space for $\delta\boldsymbol{\psi}_k$ connects to the Lie algebra $\mathbf{u}\varphi \in \mathfrak{s}^3$ (with $\mathbf{u}$ an unit vector of rotation and φ the rotated angle) with the isomorphism $(\cdot)^\wedge : \mathbb{R}^3 \mapsto \mathfrak{s}^3$. Then, the Lie algebra connects with the 3D unit-sphere $\mathcal{S}^3$ manifold through exponential mapping. The overall procedure is given by

$$\delta\boldsymbol{\psi} \in \mathbb{R}^3 \xmapsto{(\cdot)^\wedge} \mathbf{u}\varphi \in \mathfrak{s}^3 \xmapsto{\exp(\cdot)} \delta\mathbf{q} \in \mathcal{S}^3, \tag{6}$$
$$(\delta\boldsymbol{\psi})^\wedge : \begin{cases} \mathbf{u} = \frac{\delta\boldsymbol{\psi}}{\|\delta\boldsymbol{\psi}\|^2} \\ \varphi = \|\delta\boldsymbol{\psi}\|^2 \end{cases}, \exp(\mathbf{u}\varphi) : \begin{bmatrix} \cos(\varphi/2) \\ \mathbf{u}\sin(\varphi/2) \end{bmatrix}.$$

Therefore, the method $\mathbf{q}\{\boldsymbol{\psi}\}$ corresponds to the mapping between the Euclidean space and the unit quaternion one via the relationships established in (6), such that

$$\mathbf{q}\{\boldsymbol{\psi}\} \triangleq \mathbf{e}^{\mathbf{u}\varphi/\mathbf{2}} = \cos\frac{\varphi}{\mathbf{2}} + \mathbf{u}\sin\frac{\varphi}{\mathbf{2}} = \begin{bmatrix} \cos(\varphi/2) \\ \mathbf{u}\sin(\varphi/2) \end{bmatrix},$$

where $e^{(\cdot)}$ is an extension of the Euler formula, $e^{i\theta} = \cos\theta + i\sin\theta$, for imaginary numbers. In a compact expression, the composition of nominal and error state is as follows

$$\mathbf{x} = \widehat{\mathbf{x}} \oplus \delta\mathbf{x} = \begin{cases} \widehat{\mathbf{q}} & \circ & \delta\mathbf{q} \\ \widehat{\mathbf{a}} & + & \delta\mathbf{a} \\ \widehat{\mathbf{p}} & + & \delta\mathbf{p} \\ \widehat{\mathbf{v}} & + & \delta\mathbf{v} \\ \widehat{\mathbf{b}}_\omega & + & \delta\mathbf{b}_\omega \end{cases}, \tag{7}$$

$$\delta\mathbf{x} = \mathbf{x} \ominus \widehat{\mathbf{x}} \tag{8}$$

with $\circ$ the quaternion product, and $\delta\mathbf{q}$ the quaternion obtained from $\delta\boldsymbol{\psi}$ via (6). For a more detailed discussion on Lie group theory, please refer to [21, 24, 25].

Process Model: Constant-Speed Dynamics

A typical dynamical model regards a vehicle to move according to the constant-velocity model [26],

$$\mathbf{f}(\mathbf{x}_{k-1}, \boldsymbol{\omega}_{k-1}) = \begin{cases} \mathbf{q}_{k-1} \circ \boldsymbol{\Omega}_{k-1} \\ \mathbf{a}_{k-1} \\ \mathbf{p}_{k-1} + dt\ \mathbf{v}_{k-1} \\ \mathbf{v}_{k-1} \\ \mathbf{b}_{\omega,k-1} \end{cases}, \quad \text{with, } \boldsymbol{\Omega}_{k-1} = \exp(dt\ (\boldsymbol{\omega}_{k-1} - \mathbf{b}_{\omega,k-1})^{\wedge}) \tag{9}$$

where $\boldsymbol{\omega}_{k-1}$ corresponds to the three-component angular rate vector, observed at the local frame. The associated Jacobian of $\mathbf{f}(\mathbf{x}_{k-1})$ can be easily obtained

$$\mathbf{F}_k = \begin{bmatrix} \boldsymbol{\Omega}_k^{\top} & & & & -dt\ \mathbf{I}_3 \\ & \mathbf{I}_M & & & \\ & & \mathbf{I}_3 & dt\ \mathbf{I}_3 & \\ & & & \mathbf{I}_3 & \\ & & & & \mathbf{I}_3 \end{bmatrix}. \tag{10}$$

Observation Model: GNSS-Based Position and Attitude

Consider the platform configuration depicted in Fig. 1, such that one of the antennas is considered as *master* and center of the body frame, and the remaining N antennas are denoted as *slaves*. The global frame $\mathcal{G}$ is typically centered on the base station location. To eliminate atmospheric delays and other nuisance parameters, the "original" GNSS measurements at the base and slave antennas are mixed with those of the master antenna using the double difference (DD) combination [1]. The DD code and carrier phase combinations constitute the positioning- and attitude-related observations. The subscripts m, b, and $j = 1, \ldots, N$ refer to the GNSS measurements for the master, base and slave antennas, respectively, where N corresponds to the t For simplicity, the time index k is dropped for the observation description.

• *Position-related observations*

These observations, noted $\mathbf{y}_{\text{pos}}$, only involve the master antenna and are described as

$$\mathbf{y}_{\text{pos}} = \begin{bmatrix} \boldsymbol{\Phi}_{b,m} \\ \boldsymbol{\rho}_{b,m} \end{bmatrix},\ \boldsymbol{\Phi}_{b,m}, \boldsymbol{\rho}_{b,m} \in \mathbb{R}^n, \tag{11a}$$

$$[\boldsymbol{\Phi}_{b,m}]_i = -\mathbf{u}_i^{\top}\mathbf{p}_k + \lambda \cdot a_{r_i} + \epsilon_{b,m_i}, \tag{11b}$$

$$[\boldsymbol{\rho}_{b,m}]_i = -\mathbf{u}_i^{\top}\mathbf{p}_k + \varepsilon_{b,m_i}, \tag{11c}$$

where, for a generic vector $\boldsymbol{\alpha}$, $[\boldsymbol{\alpha}]_i$ and/or α_i denote the i-th DD observation, $\boldsymbol{\rho}$ and $\boldsymbol{\Phi}$ are the vector of DD code and carrier phase observations, $\mathbf{u}_i$ is the DD line-of-sight unit vector between each tracked satellite i and the base station b, λ is the GNSS carrier wavelength and $\epsilon_{b,m_i}, \varepsilon_{b,m_i}$ indicate the carrier phase and code noises for the i-th observation ($i = 1, \ldots, n$) being $n+1$ the total number of GNSS satellites. $\mathbf{a}$ contains the ambiguities and the subscript r_i in (11b) refers to the one associated with the i-th DD observation between the base station and the master antenna. The model presented in 11 applies for short baselines (i. e., distance between base station and user up to few kilometers) so that differential atmospheric delays, as well as satellite orbit errors, can be neglected.

• Attitude-related observations

Their vector of observations, denoted $\mathbf{y}_{\text{att}}$, is as follows

$$\mathbf{y}_{\text{att}}^{\top} = \left[\boldsymbol{\Phi}_{1,m}^{\top}, \ldots, \boldsymbol{\Phi}_{N,m}^{\top}, \boldsymbol{\rho}_{1,m}^{\top}, \ldots, \boldsymbol{\rho}_{N,m}^{\top}\right], \tag{12a}$$

$$\text{with } \boldsymbol{\Phi}_{j,m}, \boldsymbol{\rho}_{j,m} \in \mathbb{R}^n, j = 1, \ldots, N. \tag{12b}$$

$$[\boldsymbol{\Phi}_{j,m}]_i = -\mathbf{u}_i^{\top}\mathbf{R}(\mathbf{q})_{\mathcal{B}}\mathbf{b}_{j,m} + \lambda \cdot a_{r_{j,i}} + \epsilon_{j,m_i}, \tag{12c}$$

$$[\boldsymbol{\rho}_{j,m}]_i = -\mathbf{u}_i^{\top}\mathbf{R}(\mathbf{q})_{\mathcal{B}}\mathbf{b}_{j,m} + \varepsilon_{j,m_i}, \tag{12d}$$

where $\mathbf{R}(\mathbf{q})$ is the rotation matrix from the body frame $\mathcal{B}$ to the global navigation frame $\mathcal{G}$, derived from the associated quaternion, and ${}_{\mathcal{B}}\mathbf{b}_{\mathbf{j,m}}$ denotes the baseline vector between the j-th slave and master antennas, measured in the body frame $\mathcal{B}$ of the vehicle. The subscript $r_{j,i}$ in (12c) refers to the ambiguity associated with the i-th DD observation between the j-th slave and master antennas.

The complete vector of observations is $\mathbf{y}^{\top} = \left[\mathbf{y}_{\text{pos}}^{\top}, \quad \mathbf{y}_{\text{att}}^{\top}\right]$, the associated covariance matrix $\boldsymbol{\Sigma}$ and the Jacobian matrix $\mathbf{H}_k$ are defined in [13].

Standard Error-State KF Formulation

The ESKF adapts the EKF framework to a chosen nonlinear parametrization, here given by (7) to preserve the unit-norm quaternion constraint, while using a minimal parametrization of the covariance matrix. That is, it uses the $\oplus$ operator, instead of the standard addition, to linearize and update the system, to ensure that the estimate stays on the smooth (usually Riemannian) manifold $\mathcal{M}$. Let $\widehat{\mathbf{x}}_{k-1|k-1}$ denote the estimate at step $k-1$, and $\mathbf{P}_{k-1|k-1}$ its estimation error covariance. Then the propagation and update steps of the ESKF are given by

$$\widehat{\mathbf{x}}_{k|k-1} = \mathbf{f}(\widehat{\mathbf{x}}_{k-1|k-1}, \boldsymbol{\omega}_{k-1}) \tag{13a}$$

$$\mathbf{P}_{k|k-1} = \mathbf{F}_{k-1}\mathbf{P}_{k-1|k-1}\mathbf{F}_{k-1}^{\top} + \mathbf{Q}_{k-1}, \tag{13b}$$

$$\mathbf{S}_k = \mathbf{H}_k\mathbf{P}_{k|k-1}\mathbf{H}_k^{\top} + \boldsymbol{\Sigma}_k, \tag{13c}$$

$$\mathbf{K}_k = \mathbf{P}_{k|k-1}\mathbf{H}_k^{\top}\mathbf{S}_k^{-1}, \tag{13d}$$

$$\widehat{\mathbf{x}}_{k|k} = \widehat{\mathbf{x}}_{k|k-1} \oplus \mathbf{K}_k(\mathbf{y}_k - \mathbf{h}(\widehat{\mathbf{x}}_{k|k-1})), \tag{13e}$$

$$\mathbf{P}_{k|k} = (\mathbf{I} - \mathbf{K}_k\mathbf{H}_k)\mathbf{P}_{k|k-1}. \tag{13f}$$

The matrices $\mathbf{F}_{k-1}, \mathbf{H}_k$ represent the Jacobians of the process and observation models, $\mathbf{fh}$, with respect to the composition of nominal and error states, which is expressed using the mathematical operator $\oplus$.

3. BACKGROUND ON NONLINEAR AND ROBUST FILTERING

A Primer on the Iterated ESKF

It is well-known that, due to linearization errors, the EKF loses the optimality guarantees of the linear KF, that is, for nonlinear systems it may not provide unbiased minimum variance estimates. One way to tackle this problem is using the iterated EKF, which aims at finding the best linearization point for the measurement Jacobian at each update. It later appeared that it is in fact the application of a Gauss-Newton scheme to the following optimization problem [27]:

$$\begin{aligned} \widehat{\mathbf{x}}_{k|k} &= \underset{\mathbf{x}}{\operatorname{argmin}} \|\mathbf{x} - \widehat{\mathbf{x}}_{k|k-1}\|^2_{\mathbf{P}_{k|k-1}} + \|\mathbf{h}(\mathbf{x}) - \mathbf{y}_k\|^2_{\boldsymbol{\Sigma}_k} \\ &= \underset{\mathbf{x}}{\operatorname{argmax}}\, \mathbb{P}\left(\mathbf{x}_k | \widehat{\mathbf{x}}_{k|k-1}, \mathbf{y}_k\right). \end{aligned} \tag{14}$$

Then, applying a Gauss-Newton scheme brings the well-known iterative sequence $(\mathbf{x}_k^{(i)})_{i\geq 0}$ to compute $\widehat{\mathbf{x}}_{k|k}$. $\mathbf{x}_k^{(0)} = \widehat{\mathbf{x}}_{k|k-1}$, and, for all $i \geq 0$

$$\begin{aligned}\mathbf{x}_k^{(i+1)} &= \widehat{\mathbf{x}}_{k|k-1} \\ &+ \mathbf{K}^{(i)} \left(\mathbf{y}_k - \mathbf{h}(\mathbf{x}_k^{(i)}) + \mathbf{H}^{(i)}(\mathbf{x}_k^{(i)} - \widehat{\mathbf{x}}_{k|k-1})\right),\end{aligned} \tag{15}$$

where $\mathbf{H}^{(i)}$ is the Jacobian computed at $\mathbf{x}_k^{(i)}$, and $\mathbf{K}^{(i)}$ the Kalman gain computed from $\mathbf{P}_{k|k-1}$ and $\mathbf{H}^{(i)}$. Note that hereafter subscript i is reused to refer to the ith iteration step of the Gauss-Newton iterative process.

This scheme can be readily adapted to states living on manifolds, using the associated $\oplus, \ominus$ operators. Indeed, (14) can be reformulated for the ESKF as

$$\widehat{\mathbf{x}}_{k|k} = \underset{\mathbf{x}\in\mathcal{M}}{\operatorname{argmin}} \|\mathbf{x} \ominus \widehat{\mathbf{x}}_{k|k-1}\|^2_{\mathbf{P}_{k|k-1}} + \|\mathbf{h}(\mathbf{x}) - \mathbf{y}_k\|^2_{\boldsymbol{\Sigma}_k}. \tag{16}$$

And, in turn, the recursive formula (15) becomes [28, 29]

$$\begin{aligned}\mathbf{x}_k^{(i+1)} &= \widehat{\mathbf{x}}_{k|k-1} \\ &\oplus \mathbf{K}^{(i)} \left(\mathbf{y}_k - \mathbf{h}(\mathbf{x}_k^{(i)}) + \mathbf{H}^{(i)}(\mathbf{x}_k^{(i)} \ominus \widehat{\mathbf{x}}_{k|k-1})\right)^{2}.\end{aligned} \tag{17}$$

The iterated ESKF (I-ESKF) is particularly useful when the linearization errors of the measurement function are the main source of instability. Since $\mathbf{F}_k$ given in (10) does not depend on the estimate, this nicely fits the JPA problem. The main advantage of this formulation is that it will allow, in Section 4, to easily adapt the M-estimators derived in the vectorial case, and explained hereafter.

M-Estimators for Robust Filtering

The *robust statistics* framework provides score functions that mitigate the effect of outliers on the state estimates. A generic filter robust against outlying observations reformulates (14) as

$$\widehat{\mathbf{x}}_{k|k} = \underset{\mathbf{x}}{\operatorname{argmin}} \|\mathbf{x}-\widehat{\mathbf{x}}_{k|k-1}\|^2_{\mathbf{P}_{k|k-1}} + \|\mathbf{h}(\mathbf{x})-\mathbf{y}_k\|^2_{\bar{\boldsymbol{\Sigma}}_k}, \tag{18}$$

where $\bar{\boldsymbol{\Sigma}}_k$ is the observations' covariance matrix conditional on a set of estimated weights, such that

$$\bar{\boldsymbol{\Sigma}}_k = \boldsymbol{\Sigma}_k^{1/2}\mathbf{W}^{-1}\boldsymbol{\Sigma}_k^{\top/2}, \tag{19}$$

where $\boldsymbol{\Sigma}_k^{1/2}$ is the Cholesky factorization of $\boldsymbol{\Sigma}_k$ and $\mathbf{W}$ is a weighting matrix given by

$$\mathbf{W} = \operatorname{diag}\left[\mathbf{w}\left(\boldsymbol{\Sigma}_k^{-1/2}\big(\mathbf{y}_k - \mathbf{h}(\mathbf{x}_k)\big)\right)\right], \tag{20}$$

with $\mathbf{w}(\cdot)$ a function derived from a robust score function. The underlying idea behind robust functions is to down-weight or nullify the effect that observations not fitting the underlying model have over the actual estimates. Such robust functions can be distinguished between *monotone* or *hard-redescending*, based on their shape. Redescending functions allow for completely erasing the influence of a particular observation, at the cost of being non-convex and leading to potential numerical problems when performing inverse matrix operations. Fig. 2 illustrates the standard Huber and Tukey weighting functions, which are the most distinct examples of monotone and redescending functions, respectively. Note that robust weighting functions generally present a tuning parameter that allows controlling the *efficiency* at the normal model –i.e., how similar the mean squared error (MSE) of a robust estimator would be in comparison with an optimal maximum likelihood estimator under nominal normal distributed noises–.

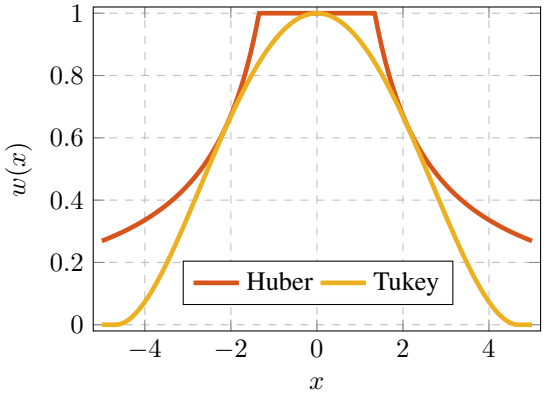

Figure 2. Weight functions associated to the Huber and Tukey robust cost functions with tuning parameters set to 95% efficiency in the Gaussian model.

The application of robust estimation over conventional KF can be realized in two manners: *i)* via Robust Information Filters (RIF) [30]; *ii)* via Generalized M-based KF (GM-KF) [31]. While GM-KF provides additional robustness against innovation outliers (i.e., those occurring during the prediction step of a filter), it does not allow using hard-redescending functions. Hereinafter, this work focuses only on RIFs.

Thus, RIF approximates (18) with an iterative procedure over the information vector $\mathbf{z}_k = \mathbf{P}_k^{-1}\mathbf{x}_k$ and information matrix $\mathbf{Z}_k = \mathbf{P}_k^{-1}$, until a certain convergence criteria is reached. Thus, for $\widehat{\mathbf{x}}^{(0)} = \widehat{\mathbf{x}}_{k|k-1}$, $\mathbf{W}^{(0)} = \mathbf{I}$ and for all $i \geq 0$

$$\begin{aligned}\mathbf{z}^{(i+1)} &= \mathbf{z}_{k|k-1} + \\ &\mathbf{H}_k^{(i)\top}\boldsymbol{\Sigma}_k^{-\top/2}\,\mathbf{W}^{(i)}\,\boldsymbol{\Sigma}_k^{-1/2}\left(\mathbf{y}_k - \mathbf{h}(\widehat{\mathbf{x}}^{(i)}) + \mathbf{H}_k^{(i)}\widehat{\mathbf{x}}_{k|k-1}\right)\end{aligned} \tag{21}$$

and updating the information matrix once the convergence is reached, as

$$\mathbf{Z}_{k|k} = \mathbf{Z}_{k|k-1} + \mathbf{H}_k^{\top}\boldsymbol{\Sigma}_k^{-\top/2}\,\mathbf{W}\,\boldsymbol{\Sigma}_k^{-1/2}\mathbf{H}_k\,. \tag{22}$$

This formulation results particularly interesting for robust filters which employ "aggressive" weighting functions. Hence, the use of such redescending functions (where the weights can become zero) may cause numerical issues within the standard robust regression KF, due to matrix inversion. Instead, the RIF formulation makes it possible to avoid these numerical issues and still exploit redescending cost functions.

Unfortunately, a formulation for the RIF compatible with state elements "living" on a manifold (e.g., such as the quaternion) is not available. In the sequel, we extend the formulation of the original RIF for its application to JPA.

[2] Some additional corrective terms, used e.g. in [28], are negligible here

4. Robust JPA Filter Formulation

Standard JPA, as introduced in [13], only relies on the conventional ESKF. Indeed, the estimates are accurate enough for the measurement Jacobian to be properly linearized. However, in the presence of outliers and when integrating inertial information, this turned out to be insufficient. In this work, we thus consider two filters for JPA, which differ from each other and the ESKF on the realization of the correction step:

- The standard I-ESKF given in (16)-(17) for the nominal Gaussian distributed case.
- A robust I-ESKF, exploiting the M-estimation RIF form, which we detail hereafter.

Just as the I-ESKF uses an adapted version of the cost function of the iterated EKF, its robust versions adapt the cost function (18) of M-estimators as

$$\widehat{\mathbf{x}}_{k|k} = \underset{\mathbf{x}\in\mathcal{M}}{\operatorname{argmin}} \|\mathbf{x}\ominus\widehat{\mathbf{x}}_{k|k-1}\|^2_{\mathbf{P}_{k|k-1}} + \|\mathbf{h}(\mathbf{x})-\mathbf{y}_k\|^2_{\boldsymbol{\Sigma}_k}, \quad (23)$$

Adapting RIFs to attitude-related problems requires converting the filters' innovation vectors to error state vectors. Taking the RIF as example case, one would provide a robust estimate by expressing the innovation over the information vector in (21) as error state, as

$$\mathbf{x}_{k|k} = \widehat{\mathbf{x}}_{k|k} \oplus \delta\mathbf{x}_{k|k}, \quad (24)$$

$$\delta\mathbf{x}_{k|k} = \mathbf{P}_{k|k}\delta\mathbf{z}_{k|k} \ , \quad (25)$$

where $\delta\mathbf{z}_{k|k}$ is a robust estimate over the change of the information vector. As in the vectorial case [18], estimating $\delta\mathbf{z}_{k|k}$ requires two cascaded iterative procedures. Indeed, consider a given fixed weight matrix $\mathbf{W}$. For this weighting, the estimate is obtained recursively, starting from $\widehat{\mathbf{x}}^{(0)} = \widehat{\mathbf{x}}_{k|k-1}$, and for $i \geq 0$ by

$$\delta\mathbf{z}^{(i+1)} = \mathbf{H}_k^{(i)\top}\boldsymbol{\Sigma}_k^{-\top/2}\mathbf{W}\boldsymbol{\Sigma}_k^{-1/2}\cdot \left(\mathbf{y}_k - \mathbf{h}(\mathbf{x}^{(i)}) + \mathbf{H}_k(\mathbf{Z}^{(i)})^{-1}\delta\mathbf{z}^{(i)}\right) \ , \quad (26)$$

$$\mathbf{Z}^{(i+1)} = \mathbf{Z}_{k|k-1} + \mathbf{H}_k^{(i)\top}\boldsymbol{\Sigma}_k^{-\top/2}\mathbf{W}\boldsymbol{\Sigma}_k^{-1/2}\mathbf{H}_k^{(i)} \quad (27)$$

$$\mathbf{x}^{(i+1)} = \mathbf{x}_{k|k-1} \oplus (\mathbf{Z}^{(i+1)})^{(-1)}\delta\mathbf{z}^{(i+1)} \quad (28)$$

Note that, in (26), $(\mathbf{Z}^{(i+1)})^{-1}\delta\mathbf{z}^{(i+1)} = \delta\mathbf{x}^{(i+1)} = \mathbf{x}_k^{(i+1)} \ominus \widehat{\mathbf{x}}_{k|k-1}$, similar to (15). The recursion (26) needs to be solved for each value of the weighting matrix, which itself is recomputed afterwards. This double recursion, given in Algorithm 1, forms the robust iterated ESKF update phase. In this paper, as explained in Section 5, we considered the Huber and Tukey robust cost functions, whose weighting functions were given in Fig. 2

5. Results

The impact of outliers on standard JPA and the proposed robust JPA was evaluated through simulation experiments. We considered a medium-sized vehicle (e.g., a small ship, a small plane or a car), containing 3 slave antennas in addition to the master one, and observing ten satellites (the skyplot shown in figure 3 coincides with [32]). Each slave antenna is assumed to be separated from the master antenna by a distance $\|{}_{\mathcal{B}}\widehat{\mathbf{b}}_{j,m}\| = 1$ m. The vehicle starts at a distance of 5 km from the base station, and its velocity follows a random walk as well as the gyroscope biases. GNSS data was obtained at 1 Hz, and recorded for 1000 s. The number of Monte Carlo runs is set to 100. Stochastic modelling for the undifferenced GNSS observations follows a satellite elevation-dependent model [33], with the zenith-referenced code and carrier standard deviations given in Table 1.

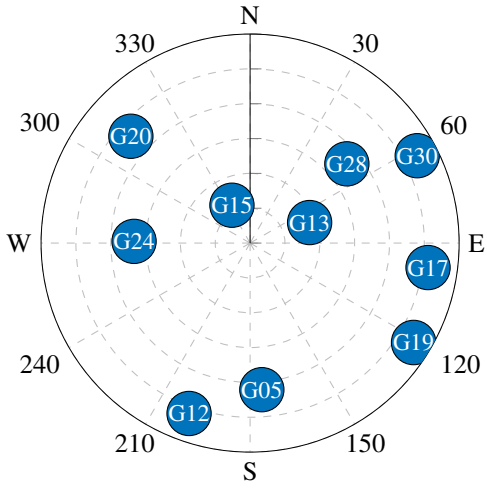

Figure 3. Skyplot for the simulated constellation.

Within the simulated trajectory, we defined two types of behaviours, a nominal one and a corrupted one (indicated as shaded gray areas in upcoming figures). In the grey zones, we aimed for 20% of outliers, so satellites G20 and G24 were corrupted across all antennas. In this case, their phase noise distribution does not change but they are affected by a cycle slip.

A total of four filters have been evaluated, which we can be categorized as (a) iterative ESKF (I-ESKF), which includes an ideal I-ESKF (i.e., a filter with information on which observations are outliers and sets the best possible solution by discarding those degraded observations) and an I-ESKF (i.e., a classical filter heavily affected by the presence of outliers); and (b) robust filters, as defined in Section 3, based on Huber and Tukey cost functions.

Algorithm 1 Robust Iterated ESKF Correction Step

Input: Observations: $\mathbf{y}, \boldsymbol{\Sigma}$,
Robust-estimator parameters: $w(\cdot), c$
Predicted estimate: $\widehat{\mathbf{x}}_{k|k-1}, \mathbf{P}_{k|k-1}$
Output: Updated estimate $\widehat{\mathbf{x}}_{k|k}, \mathbf{P}_{k|k}$

Initialize $\mathbf{W}^{(0)} = \mathbf{I}$, $\widehat{\mathbf{x}}^{(0)} = \widehat{\mathbf{x}}_{k|k-1}$,
for $p = 1, \ldots$ until convergence **do**
Solve (23) via (26)-(28) to obtain $\widehat{\mathbf{x}}^{(p)}, \mathbf{Z}^{(p)}$
Update the weighting matrix:
$\mathbf{W}^{(p)} = \operatorname{diag}\left(\mathbf{w}\left(\boldsymbol{\Sigma}_k^{-1/2}(\mathbf{y} - \mathbf{h}(\widehat{\mathbf{x}}^{(p)}))\right)\right)$
end for
$\widehat{\mathbf{x}}_{k|k} = \widehat{\mathbf{x}}^{(p)}$
$\mathbf{P}_{k|k} = \left(\mathbf{Z}^{(p)}\right)^{-1}$

We computed the root mean squared error (RMSE) of the position, angles, and bias, in addition to the cumulative distribution function (CDF) for the positioning error. Moreover, we assessed the efficiency of the robust filters in the nominal case, defined here as the relative performance of a particular estimator with respect to the I-ESKF in nominal conditions under normal-distributed noise. Such metric is defined for an exact noise model F and a target estimator $\hat{\theta}(F)$ as the ratio in asymptotic variance between the optimal estimator (i.e., the MLE for the F model) and the target estimator, as

$$\text{Eff}\left(\hat{\theta}(F), F\right) = \frac{\text{var}\left(\hat{\theta}_{\text{MLE}}(F), F\right)}{\text{var}\left(\hat{\theta}(F), F\right)}, \tag{29}$$

such that the efficiency is delimited by $0 \leq \text{Eff}\left(\hat{\theta}(F), F\right) \leq 1$.

Table 1. Monte Carlo simulation parameters.

Initial std. dev.	Position: 10 [m] Velocity: $[2, 2, 2 \cdot 10^{-3}]$ [m/s] Attitude: 10 [deg] Gyroscope bias: $2 \cdot 10^{-3}$ $[^\circ/\sqrt{s^3}]$ Ambiguities: 4 [cycles]
Process noise std. dev.	Velocity (East-North-Up): $[1, 1, 10^{-3}]$ [m/s] Gyroscope: $2 \cdot 10^{-3}$ $[^\circ/\sqrt{s^3}]$ Bias random walk: $2 \cdot 10^{-5}$ $[^\circ/(\sqrt{s^3})]$ Ambiguities: $1 \cdot 10^{-16}$ [cycles/$\sqrt{s}$]
Obs. noise std. dev.	Code zenith-referenced: 0.3 [m] Carrier phase zenith-referenced: 3 [mm]
Outliers rate	20%
Cost func. parameters	Huber: 1.345 Tukey: 4.685

Nominal case:

First, a nominal (outlier-free) case was considered, in order to assess the efficiency of the different robust methods [34]. Indeed, robust solutions are expected to have lower performance in nominal cases, so their design should allow them to be close-to-optimal. Quantitatively, this means having an efficiency as close as possible to 1. As shown in Fig. 4, both filters manage to achieve it.

Non-nominal case:

After validating the efficiency of the proposed filters, we can analyse their behavior in a non-nominal scenario. We thus considered the contamination of the measurements from 20% of the satellites. The RMSE of the position, attitude and gyroscope bias for each filter is presented in figure 6. The moments where outliers are present are illustrated by the grey zones.

Since attitude and gyroscope bias are less affected by these outliers, the I-ESKF still manages to correctly estimate them, and slightly better than the robust filters. However, its performance for the position is significantly degraded when outliers are present. Indeed, these observations get directly affected by the outliers, and the I-ESKF does not recover afterwards when conditions are back to nominal. The robust filters, on the other hand, achieve much better performance, especially during the outliers intervals. Interestingly, they show jumps in

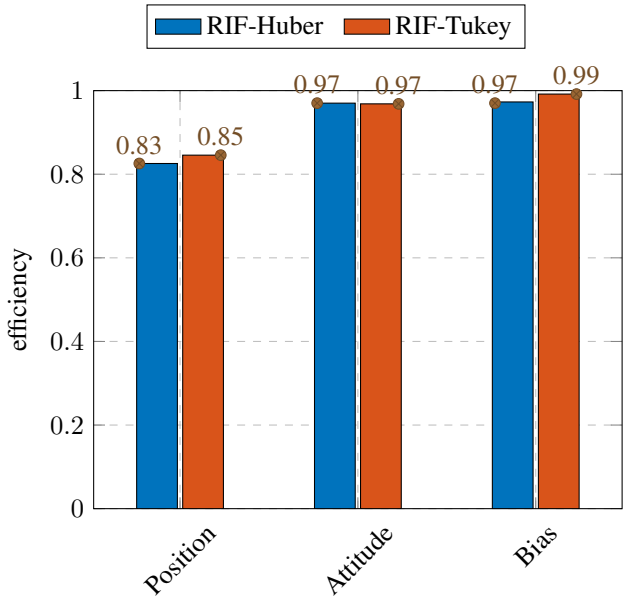

Figure 4. **Nominal case: Efficiency over time for robust ESKFs.**

the error when the conditions go back to nominal, but manage to recover from them. More intriguing, using the Tukey cost function performs actually better in non-nominal case. A first intuition could be that the outliers actually help it identify the corrupted satellites since it can put weights to zero. However, this needs further research to fully understand this behavior.

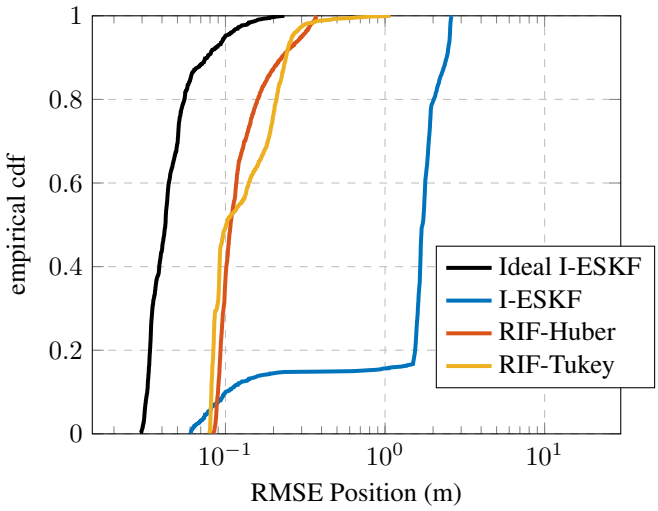

Figure 5. **Non-nominal case: Empirical cumulative distribution function (CDF) of the float positioning errors.**

6. Conclusion

In this paper, we elaborated on the recent JPA estimation framework, to propose a robust counterpart to it in order to alleviate the presence of potential outliers. To do so, we built on the robust estimation methodology, which had been already applied to RTK estimation. However, fusing JPA and robust estimators brought the necessity of better handling nonlinearities, in an iterative manner. We thus proposed

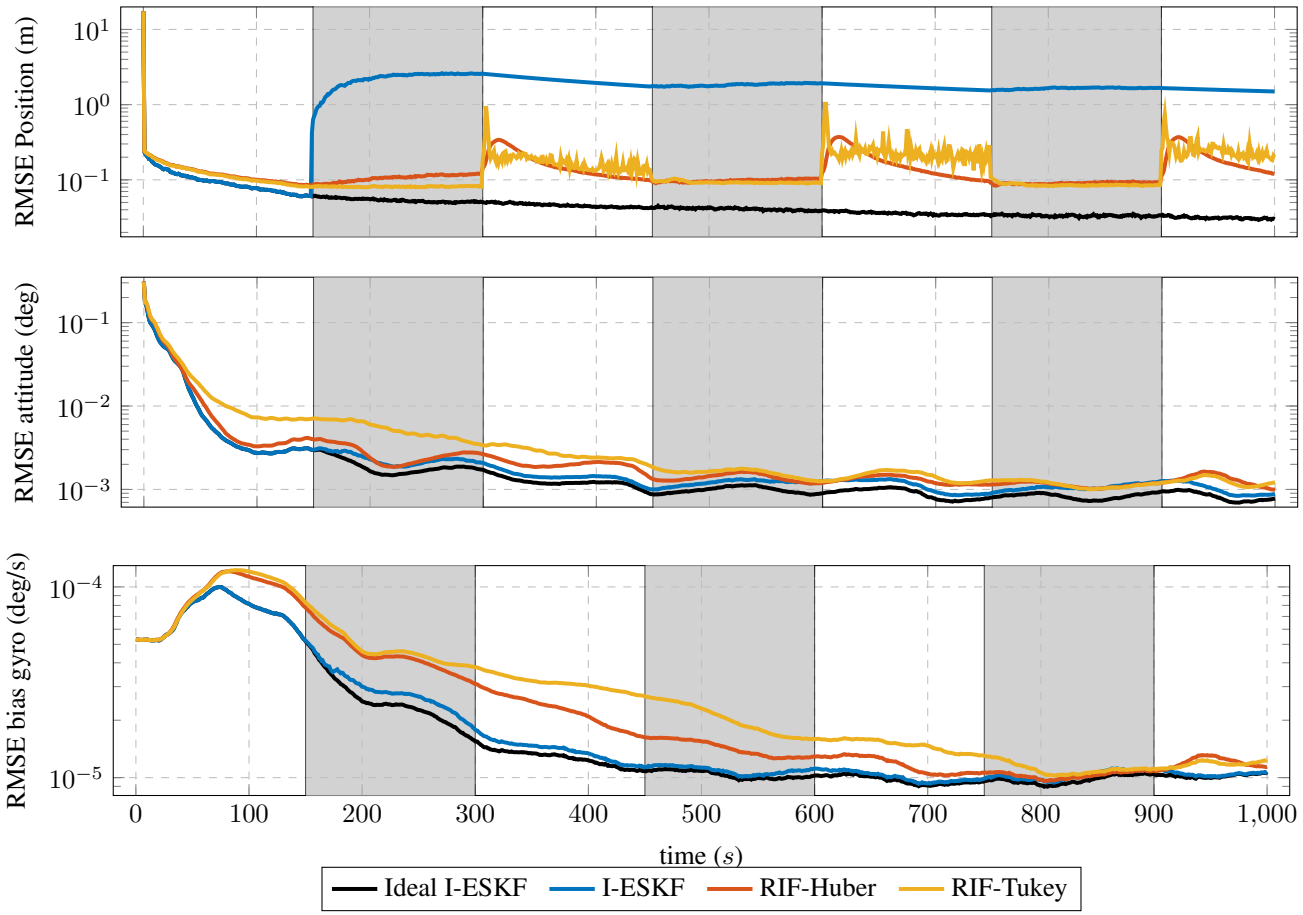

Figure 6. **Non-nominal case: Evolution of the root mean squared error (RMSE) for the float solution over time.**

to use a robust iterated ESKF, whose update uses an inner reweighting loop. The impact of outliers on standard JPA, and the capacity of the proposed filter to mitigate them, were illustrated on numerical examples. It appeared that the robust filters are less impacted by the outliers and that they manage to quickly recover from them, contrary to standard JPA.

ACKNOWLEDGMENTS

This work has been partially supported by the DGA/AID project 2019.65.0068.00.470.75.01.

REFERENCES

[1] P. J. G. Teunissen and O. Montenbruck, Eds., *Handbook of Global Navigation Satellite Systems*. Switzerland: Springer, 2017.

[2] V. W. Spinney, "Applications of the Global Positioning System as an Attitude Reference for Near Earth Users," *Navigation*, 1976.

[3] A. Hauschild, O. Montenbruck, and R. B. Langley, "Flight Results of GPS-Based Attitude Determination for the Canadian CASSIOPE Satellite," *Navigation*, vol. 67, no. 1, pp. 83–93, 2020.

[4] A. Hauschild, "GNSS Yaw Attitude Estimation: Results for the Japanese Quasi-Zenith Satellite System Block-II Satellites using Single-or Triple-Frequency Signals from Two Antennas," *Navigation*, vol. 66, no. 4, pp. 719–728, 2019.

[5] P. J. G. Teunissen, G. Giorgi, and P. J. Buist, "Testing of a New Single-Frequency GNSS Carrier Phase Attitude Determination Method: Land, Ship and Aircraft Experiments," *GPS Solutions*, vol. 15, no. 1, pp. 15–28, 2011.

[6] F. Aghili and A. Salerno, "Driftless 3-D attitude determination and positioning of mobile robots by integration of IMU with two RTK GPSs," *IEEE/ASME Transactions on Mechatronics*, vol. 18, no. 1, pp. 21–31, 2011.

[7] J. Schneider, C. Eling, L. Klingbeil, H. Kuhlmann, W. Förstner, and C. Stachniss, "Fast and Effective Online Pose Estimation and Mapping for UAVs," in *Proc. of the IEEE International Conference on Robotics and Automation (ICRA)*, 2016, pp. 4784–4791.

[8] L. Meyer *et al.*, "The MADMAX Data Set for Visual-Inertial Rover Navigation on Mars," *Journal of Field Robotics*, March 2021.

[9] G. Giorgi and P. J. Teunissen, "Carrier phase GNSS attitude determination with the multivariate constrained LAMBDA method," in *2010 IEEE Aerospace Conference*. IEEE, 2010, pp. 1–12.

[10] G. Giorgi, P. J. Teunissen, and T. P. Gourlay, "Instantaneous global navigation satellite system (gnss)-based attitude determination for maritime applications," *IEEE Journal of oceanic engineering*, vol. 37, no. 3, pp. 348–362, 2012.

[11] D. Medina, V. Centrone, R. Ziebold, and J. García, "Attitude determination via GNSS carrier phase and inertial aiding," in *Proceedings of the 32nd International Technical Meeting of the Satellite Division of The Institute of Navigation (ION GNSS+ 2019)*, 2019, pp. 2964–2979.

[12] P. J. Teunissen, "A-PPP: Array-aided Precise Point Positioning with Global Navigation Satellite Systems," *IEEE Transactions on Signal Processing*, vol. 60, no. 6, pp. 2870–2881, 2012.

[13] D. Medina, J. Vilà-Valls, A. Heßelbarth, R. Ziebold, and J. García, "On the Recursive Joint Position and Attitude Determination in Multi-Antenna GNSS Platforms," *Remote Sensing*, vol. 12, no. 12, 2020.

[14] N. L. Knight and J. Wang, "A comparison of outlier detection procedures and robust estimation methods in GPS positioning," *The Journal of Navigation*, vol. 62, no. 4, pp. 699–709, 2009.

[15] O. G. Crespillo, D. Medina, J. Skaloud, and M. Meurer, "Tightly coupled GNSS/INS integration based on robust M-estimators," in *2018 IEEE/ION Position, Location and Navigation Symposium (PLANS)*, April 2018.

[16] D. Medina, H. Li, J. Vilà-Valls, and P. Closas, "Robust Statistics for GNSS Positioning under Harsh Conditions: A Useful Tool?" *Sensors*, vol. 19, no. 24, p. 5402, 2019.

[17] H. Li, D. Medina, J. Vilà-Valls, and P. Closas, "Robust Kalman Filter for RTK Positioning Under Signal-Degraded Scenarios," in *Proceedings of the 32nd International Technical Meeting of the Satellite Division of the Institute of Navigation (ION GNSS+ 2019), Miami, FL, USA*, 2019, pp. 16–20.

[18] D. Medina, H. Li, J. Vilà-Valls, and P. Closas, "Robust Filtering Techniques for RTK Positioning in Harsh Propagation Environments," *Sensors*, vol. 21, no. 4, p. 1250, 2021.

[19] F. L. Markley, "Attitude Error Representations for Kalman Filtering," *Journal of Guidance, Control, and Dynamics*, vol. 26, no. 2, pp. 311–317, March 2003. [Online]. Available: https://doi.org/10.2514%2F2.5048

[20] J. L. Crassidis, F. L. Markley, and Y. Cheng, "Survey of nonlinear attitude estimation methods," *Journal of Guidance, Control, and Dynamics*, vol. 30, no. 1, pp. 12–28, 2007.

[21] T. D. Barfoot, *State Estimation for Robotics*. Cambridge University Press, 2017.

[22] S. I. Roumeliotis, G. S. Sukhatme, and G. A. Bekey, "Circumventing Dynamic Modeling: Evaluation of the Error-State Kalman Filter Applied to Mobile Robot Localization," in *Proc. of the IEEE International Conference on Robotics and Automation*, 1999, pp. 1656–1663 vol.2.

[23] J. Solà, "Quaternion Kinematics for the Error-State Kalman Filter," *CoRR*, vol. abs/1711.02508, 2017. [Online]. Available: http://arxiv.org/abs/1711.02508

[24] J. Stillwell, *Naive Lie Theory*. Springer Sci. & Business Media, 2008.

[25] J. Sola, J. Deray, and D. Atchuthan, "A Micro Lie Theory for State Estimation in Robotics," *arXiv preprint arXiv:1812.01537*, 2018.

[26] Y. Bar-Shalom, X.-R. Li, and T. Kirubarajan, *Estimation with Applications to Tracking and Navigation*. John Wiley & Sons, 2001.

[27] B. M. Bell and F. W. Cathey, "The iterated Kalman filter update as a Gauss-Newton method," *IEEE Transactions on Automatic Control*, vol. 38, no. 2, pp. 294–297, Feb 1993.

[28] G. Bourmaud, R. Mégret, A. Giremus, and Y. Berthoumieu, "From Intrinsic Optimization to Iterated Extended Kalman Filtering on Lie Groups," *J. Math. Imaging Vis.*, vol. 55, no. 3, pp. 284–303, Jul. 2016. [Online]. Available: http://dx.doi.org/10.1007/s10851-015-0622-8

[29] P. Chauchat, A. Barrau, and S. Bonnabel, "Invariant Smoothing on Lie Groups," in *IEEE/RSJ International Conference on Intelligent Robots and Systems, IROS 2018*, Madrid, Spain, Oct. 2018. [Online]. Available: https://hal.archives-ouvertes.fr/hal-01725847

[30] L. Chang and K. Li, "Unified Form for the Robust Gaussian Information Filtering based on M-estimate," *IEEE Signal Processing Letters*, vol. 24, no. 4, pp. 412–416, 2017.

[31] M. A. Gandhi and L. Mili, "Robust Kalman Filter based on a Generalized Maximum-Likelihood-type Estimator," *IEEE Transactions on Signal Processing*, vol. 58, no. 5, pp. 2509–2520, 2009.

[32] D. Medina, J. Vilà-Valls, E. Chaumette, F. Vincent, and P. Closas, "Cramér-Rao Bound for a Mixture of Real- and Integer-Valued Parameter Vectors and Its Application to the Linear Regression Model," *Signal Processing*, vol. 179, 2021.

[33] H.-J. Eueler and C. C. Goad, "On Optimal Filtering of GPS Dual Frequency Observations Without Using Orbit Information," *Bulletin géodésique*, vol. 65, no. 2, pp. 130–143, 1991.

[34] P. J. Huber, "Robust Regression: Asymptotics, Conjectures and Monte Carlo," *The Annals of Statistics*, vol. 1, no. 5, pp. 799 – 821, 1973. [Online]. Available: https://doi.org/10.1214/aos/1176342503

Andrea Bellés *received her B.S. in Aerospace Engineering from Universitat Politècnica de Catalunya (EETAC-UPC), Spain, in 2019. Currently she pursues her M.S. in Aerospace Systems, Navigation and Telecommunications at the École Nationale de l'Aviation Civile (ENAC), University of Toulouse, France; and she is carrying out her M.S. thesis at the Institute of Communications and Navigation of the German Aerospace Center.*

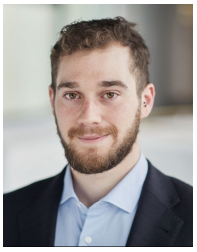

Daniel Medina *received his B.S. in Electrical Engineering from the University of Malaga and his M.S. in Computer Science from Charles III University of Madrid in 2014 and 2016 respectively. Currently he pursues his PhD on multi – sensor fusion for precise positioning and attitude determination. Since 2016, is a research fellow at the Institute of Communications and Navigation of the German Aerospace Center.*

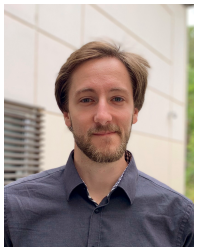

Paul Chauchat *received the engineering degree in Applied Mathematics from Ecole CentraleSupélec, Gif-sur-Yvette, France, in 2016, and the Ph.D. degree in Computer Science from Ecole des Mines ParisTech, Paris, France, in 2020. He is currently a Postdoctoral researcher at ISAE-Supaéro, working on robust linear and nonlinear state estimation with applications to navigation and remote sensing.*

Jordi Vilà-Valls *is Associate Professor at the Institut Supérieur de l'Aéronautique et de l'Espace (ISAE-SUPAERO), University of Toulouse, France. He received the MS in Electrical Engineering from both Universitat Politècnica de Catalunya (UPC), Spain, and Grenoble Institute of Technology (INPG), France, in 2006, and the PhD in Signal Processing from INPG in 2010. His primary areas of interest include statistical signal processing, estimation and detection theory, nonlinear Bayesian inference and robust filtering, with applications to localization, tracking, navigation and remote sensing.*